Size-Dependent Extinction Coefficients of PbS Quantum Dots

Ludovico Cademartiri,[†] Erica Montanari,[‡] Gianluca Calestani,[‡] Andrea Migliori,[§]
Antonietta Guagliardi,[⊥] and Geoffrey A. Ozin*,[†]

*Contribution from the Materials Chemistry Research Group, Lash Miller Chemical Laboratories,
Department of Chemistry, University of Toronto, 80 St. George Street, Toronto, Ontario M5S
3H6, Canada, Dipartimento di Chimica GIAF, Università di Parma, Via G. P. Usberti 17/a,
I-43100 Parma, Italy, Consiglio Nazionale delle Ricerche, CNR-IMM, Area della Ricerca di
Bologna, Via Gobetti 101, I-40126 Bologna, Italy, and Consiglio Nazionale delle Ricerche,
Istituto di Cristallografia (CNR-IC),Via Amendola 122/O, I-70126 Bari, Italy*

Received May 12, 2006; E-mail: gozin@chem.utoronto.ca

Abstract: We report here on a detailed study on PbS colloidal quantum dots. A characterization via X-ray diffraction (XRD) and high-resolution transmission electron microscopy (HRTEM) allowed us to reliably determine the diameter and the shape of the nanocrystals. These data, together with second-derivative analysis of the absorption spectra, allowed us to determine the size dependence of seven transitions in the absorption spectrum; some of these transitions were identified on the basis of their normalized confinement energy. The size dependence of the first excitonic transition was best modeled by a four-band envelope approach which considers the anisotropy of the band edges (Andreev, A. D.; Lipovskii, A. A. *Phys. Rev. B: Condens. Matter Mater. Phys.* **1999**, *59*, 15402−15404). The extinction coefficients were calculated using concentrations obtained from inductively coupled plasma atomic emission spectrometry (ICP-AES), and their size dependence was found to follow a power law with exponent equal to ∼2.5. In contrast with what was expected from the effective mass approximation, the *per particle* absorption cross section of the lowest transition was found to be strongly dependent on the particle size.

Introduction

The exponentially increasing research in nanotechnology is producing a wealth of new materials for which much of the "basic" characterization is missing. There are many reasons for this lack of data about nanostructures; for example, reported syntheses are often not sufficiently reproducible, or the resulting material does not have the quality (often in terms of monodispersity, surface composition, or colloidal stability) or the purity that is required for many in-detail studies.

One of the consequences is that, more and more, advanced experiments are slowed by the unavailability of proper data regarding some basic properties of these nanomaterials. For example, for most of the available nanocrystals, it is not possible to know easily and accurately the concentration of a solution of a given absorbance, as the extinction coefficients have never been measured and, in many cases, are strongly dependent on size. For anybody who is working on the applications of colloidal quantum dots, this has always been a source of distress, since many projects require a very good estimate for the concentration of a quantum dot solution if one wants to avoid lengthy trial-and-error procedures which are inevitably going to lack reproducibility. The in situ study of nucleation and growth,[2] the development of SILAR-type core−shell procedures,[3] the formation of nanocrystal−polymer composites,[4] and the self-assembly of nanocrystal superlattices[5] are examples of projects which would greatly benefit from a knowledge of the extinction coefficient.

The relevance of the extinction coefficient, and especially its size dependence, is not only limited to technical issues.[6,7] Much is known about the quantum size effect on the transition energies, but much less is experimentally known about the quantum size effect on the extinction coefficient which, as correctly stated by Wang and Herron, is one of the two most important consequences of carrier confinement.[6]

There are many reasons for the scarcity of extinction coefficient data from colloidal nanocrystals. The product needs to be pure, with no excess precursors dissolved in the solution, but it is often difficult, and sometimes impossible, to purify nanocrystal to this extent without compromising their colloidal stability.[8] The solution also needs to be diluted for UV−VIS spectroscopy so that the absorbance is linear with concentration,

[†] University of Toronto.
[‡] Universitá di Parma.
[§] Consiglio Nazionale delle Ricerche, CNR-IMM.
[⊥] Consiglio Nazionale delle Ricerche, CNR-IC.
(1) Andreev, A. D.; Lipovskii, A. A. *Phys. Rev. B: Condens. Matter Mater. Phys.* **1999**, *59*, 15402−15404.
(2) Qu, L.; Yu, W. W.; Peng, X. *Nano Lett.* **2004**, *4*, 465−469.

(3) Li, J. J.; Wang, Y. A.; Guo, W.; Keay, J. C.; Mishima, T. D.; Johnson, M. B.; Peng, X. *J. Am. Chem. Soc.* **2003**, *125*, 12567−12575.
(4) Wang, Y.; Suna, A.; Mahler, W.; Kasowski, R. *J. Chem. Phys.* **1987**, *87*, 7315−7322.
(5) Shevchenko, E. V.; Talapin, D. V.; Kotov, N. A.; O'Brien, S.; Murray, C. B. *Nature* **2006**, *439*, 55−59.
(6) Wang, Y.; Herron, N. *J. Phys. Chem.* **1991**, *95*, 525.
(7) Brus, L. *J. Phys. Chem.* **1986**, *90*, 2555−2560.
(8) Xie, R. G.; Kolb, U.; Li, J. X.; Basche, T.; Mews, A. *J. Am. Chem. Soc.* **2005**, *127*, 7480−7488.

and many nanocrystals are unstable under such dilute conditions, most probably for the same reasons that they are unstable in very pure solvents. The nanocrystals have to be stable in size, without ripening[9] or etching[10] over time, as the set of measurements necessary for the determination of the extinction coefficient is lengthy. The nanocrystals in the size series have to be directly comparable in terms of shape, size distribution, and composition, properties which require great reproducibility in the reaction or large-scale syntheses. The sizes of the nanocrystals have to be known with extreme precision, which means lengthy analysis at the HRTEM, having to deal with the uncertainty of the *K* parameter in the Scherrer formula for determining crystal size from XRD peak broadening,[11] or having to disperse the particles in polymers for SAXS characterization.[12] So, it is necessary to have a very reproducible synthesis of highly stable and purifiable nanocrystals before embarking on this set of experiments.

In the present work, we focused on PbS colloidal nanocrystals for which we optimized a highly robust and large-scale synthesis.[13] The advantage of this synthesis is that the Pb precursor is insoluble in hexane, the solvent in which the nanocrystals are dispersed, allowing us to efficiently remove the excess precursor. These nanocrystals are near-infrared (NIR)-emitting quantum dots having high quantum efficiency and very good monodispersity. The main limitation of our synthesis, when compared to some routes reported before,[10,14−16] is its apparent inability to produce very small nanocrystals (diameter < 4 nm).

Our focus on NIR-emitting nanocrystals is mostly due to their applicability as light sources for telecommunication,[17] as biological labels,[18] and as light harvesters.[19,20] In the case of lead chalcogenides, though, our interest is motivated not only by the wavelength range in which they emit but also by their unique properties, including large dielectric constants[21] and Bohr radii,[21] efficient multiple exciton generation,[21,22] and large carrier mobility.[23] The applicability of lead chalcogenide nanocrystals in biotagging remains, at the moment, questionable due to the unavailability of efficient core−shell architectures for these materials and to concerns about the toxicity of Pb-based nanomaterials.

The determination of the extinction coefficient in colloidal quantum dots has been performed using different methods, yielding somewhat inconsistent results. The elemental analysis used by Schmelz et al.[24] gave a linear dependence of the molar extinction coefficient on the volume of small CdSe nanocrystals, even though the fit was not unambiguous, probably due to polydispersity of the size distribution. Striolo et al.[25] used osmotic methods to determine the molar extinction coefficient of CdSe nanocrystals, showing a rough agreement with the data reported by Schmelz et al. Bawendi's group determined the absorption cross section of a size series of highly monodisperse CdSe nanocrystals by gravimetric methods, finding a linear dependence on the size of the oscillator strength *per particle* for the lowest interband transition,[26] where theoretical arguments would have predicted it to be independent.[27,28] Peng's group conducted a very detailed characterization of high-quality CdS, CdSe, and CdTe nanocrystals in a wide size range, using elemental analysis and controlled etching to determine the extinction coefficient for the peak value of the lowest interband transition, which was found to be proportional to the second-to-third power of the radius.[29] Early work on water-soluble CdS[30] and CdTe nanocrystals[31] showed a linear dependence of the molar extinction coefficient on the volume of the particles. More recent results on InAs quantum dots showed a size independence of the *per particle* oscillator strength,[32] as predicted by theory. The inconsistency of such results is also often complicated by the variety of techniques and sample preparations that have been employed.

Every method for the calculation of extinction coefficients for nanocrystals has its advantages and drawbacks. We decided to use elemental analysis of digested nanocrystals and a combination of HRTEM and XRD techniques to determine accurately the size of the nanocrystals, as this approach would allow us to get the smallest error in the final result.

In this work, we calculated the extinction coefficients (*per particle*) as well as the absorption cross sections for a size series of PbS nanocrystals dispersed in hexane. We also determined the energies for seven discernible transitions as a function of size by using second-derivative analysis of the absorption spectra. The sizes were determined by independent XRD and TEM techniques, while the concentrations of Pb in solution of digested quantum dots were determined by ICP-AES.

Experimental Section

PbS Nanocrystal Synthesis and Purification. All the nanocrystals analyzed in this report were obtained from the same reaction, thus providing a better uniformity in the results. The nanocrystals were prepared according to a previously published procedure.[13] One gram of $PbCl_2$ (98%) was poured into 1.93 g of stirring oleylamine (OLA) under N_2 flow. The mixture was heated to 100 °C, the reaction flask sealed with a rubber septum, and vacuum applied for 5 min. The flask

(9) Zhao, X. S.; Gorelikov, I.; Musikhin, S.; Cauchi, S.; Sukhovatkin, V.; Sargent, E. H.; Kumacheva, E. *Langmuir* **2005**, *21*, 1086−1090.
(10) Hines, M. A.; Scholes, G. D. *Adv. Mater.* **2003**, *15*, 1844−1849.
(11) Borchert, H.; Shevchenko, E. V.; Robert, A.; Mekis, I.; Kornowski, A.; Grubel, G.; Weller, H. *Langmuir* **2005**, *21*, 1931−1936.
(12) Murray, C. B.; Kagan, C. R.; Bawendi, M. G. *Annu. Rev. Mater. Res.* **2000**, *30*, 545−610.
(13) Cademartiri, L.; Bertolotti, J.; Sapienza, R.; Wiersma, D. S.; Kitaev, V.; Ozin, G. A. *J. Phys. Chem. B* **2006**, *110*, 671−673.
(14) Bakueva, L.; Gorelikov, I.; Musikhin, S.; Zhao, X. S.; Sargent, E. H.; Kumacheva, E. *Adv. Mater.* **2004**, *16*, 926.
(15) Warner, J. H.; Thomsen, E.; Watt, A. R.; Heckenberg, N. R.; Rubinutein-Dunlop, H. *Nanotechnology* **2005**, *16*, 175−179.
(16) Nenadovic, M. T.; Rajh, T.; Micic, O. I. *J. Phys. Chem.* **1985**, *89*, 397−399.
(17) Wise, F. W. *Acc. Chem. Res.* **2000**, *33*, 773−780.
(18) Medintz, I. L.; Goldman, E. R.; Uyeda, H. T.; Mattoussi, H. *Nat. Mater.* **2005**, *4*, 435−446.
(19) Schaller, R. D.; Klimov, V. I. *Phys. Rev. Lett.* **2004**, *92*, 186601-1.
(20) McDonald, S. A.; Konstantatos, G.; Zhang, S. G.; Cyr, P. W.; Klem, E. J. D.; Levina, L.; Sargent, E. H. *Nat. Mater.* **2005**, *4*, 138-U14.
(21) Murphy, J. E.; Beard, M. C.; Norman, A. G.; Ahrenkiel, S. P.; Johnson, J. C.; Yu, P.; Micic, O. I.; Ellingson, R. J.; Nozik, A. J. *J. Am. Chem. Soc.* **2006**, *128*, 3241−3247.
(22) Ellingson, R. J.; Beard, M. C.; Micic, O. I.; Nozik, A. J.; Johnson, J. C.; Yu, P.; Shabaev, A.; Efros, A. L. *Nano Lett.* **2005**, *5*, 865−871.
(23) Talapin, D. V.; Murray, C. B., *Science* **2005**, *310*, 86−89.

(24) Schmelz, O.; Mews, A.; Basche, T.; Herrmann, A.; Mullen, K. *Langmuir* **2001**, *17*, 2861−2865.
(25) Striolo, A.; Ward, J.; Prausnitz, J. M.; Parak, W. J.; Zanchet, D.; Gerion, D.; Milliron, D.; Alivisatos, A. P. *J. Phys. Chem. B* **2002**, *106*, 5500−5505.
(26) Leatherdale, C. A.; Woo, W. K.; Mikulec, F. V.; Bawendi, M. G. *J. Phys. Chem. B* **2002**, *106*, 7619−7622.
(27) Efros, A. L.; Efros, A. L. *Sov. Phys. Semicond.* **1982**, *16*, 772−775.
(28) Brus, L. E. *J. Chem. Phys.* **1984**, *80*, 4403−4409.
(29) Yu, W. W.; Qu, L.; Guo, W.; Peng, X. *Chem. Mater.* **2003**, *15*, 2854−2860.
(30) Vossmeyer, T.; Katsikas, L.; Giersig, M.; Popovic, I. G.; Diesner, K.; Chemseddine, A.; Eychmuller, A.; Weller, H. *J. Phys. Chem.* **1994**, *98*, 7665−7673.
(31) Rajh, T.; Micic, O. I.; Nozik, A. J. *J. Phys. Chem.* **1993**, *97*, 11999−12003.
(32) Yu, P. R.; Beard, M. C.; Ellingson, R. J.; Ferrere, S.; Curtis, C.; Drexler, J.; Luiszer, F.; Nozik, A. J. *J. Phys. Chem. B* **2005**, *109*, 7084−7087.

was reopened, the N_2 flow restored, and the temperature increased to 120 °C, where it was left for 30 min, always under vigorous stirring. During that time, the $PbCl_2$–OLA mixture turned into a highly viscous, homogeneous gel. The S precursor solution was prepared in the meantime by adding 0.0115 g of elemental S to 0.2 g of OLA. Dissolution of the elemental sulfur can be completed by ultrasonication and gentle heating at 80 °C in an oven with frequent shaking. The S solution was then injected at room temperature into the stirring $PbCl_2$–OLA gel, and nucleation proceeded almost instantaneously. The temperature was stabilized to 100 °C for the subsequent growth.

The samples were collected with a syringe at different time intervals spanning 7 h during the growth and rapidly quenched into cold hexane in 15 mL centrifuge tubes. The tubes were centrifuged for 15 min at 3000 rpm to precipitate the excess $PbCl_2$ precursor. A minimum amount of ethanol was added to the supernatant to induce precipitation of the nanocrystals. The solutions were centrifuged, the supernatant was discarded, and the precipitate was redispersed in hexane. To further purify the nanocrystals, we added 200% in volume of oleic acid (OA) to the hexane dispersions of PbS nanocrystals, and the samples were shaken for 5 min, after which they were centrifuged. The supernatant was discarded, and the nanocrystals were redispersed into hexane. The nanocrystals were then further precipitated twice with ethanol and redispersed in hexane to remove any further trace of ligands. The nanocrystals dispersions were dried under N_2 and redispersed in hexane to remove any trace of ethanol from the solution. To be sure that all $PbCl_2$ was precipitated from solution ($PbCl_2$ is insoluble in hexane), we stored the samples for 6 months. After that time, all traces of $PbCl_2$ had precipitated, and they were separated by centrifugation at 3000 rpm for 1 h. All chemicals were purchased from Aldrich unless otherwise stated.

UV–Vis–NIR Characterization. The nanocrystal dispersions were diluted to a known volume, having optical densities at the first exciton peak of about 0.2. The absorption spectra were measured in the range between 500 and 1700 nm with a Perkin-Elmer Lambda 900 UV–vis–NIR spectrometer.

ICP-AES Characterization. These experiments were performed at the Analest facilities at the University of Toronto. A known volume of nanocrystal dispersions of known absorbance was dried with N_2 and digested with a HNO_3/H_2O_2 mixture on a hotplate. The obtained clear solutions were diluted to 10 mL with Millipore water. The four calibration standards were prepared with $Pb(NO_3)_2$, giving a linear fit with correlation coefficient of 0.99996. The strongest emission line for Pb (220.353 nm) was chosen for the calculation of the concentrations.

TEM Characterization. Transmission electron microscopy characterization was performed using a Philips TECNAI F20 microscope, operating at 200 keV, equipped with both a high-angle annular dark field (HAADF) detector and a slow-scan CCD camera.

The specimens were prepared by depositing a droplet of the colloidal suspension on a thin carbon film supported by a copper grid.

XRD Characterization. Powder XRD characterization was performed by a Thermo ARL X'tra powder diffractometer, equipped with a solid-state thermo electron detector. Samples were prepared by evaporating the suspensions on a zero-background sample holder. Diffraction patterns were collected in the 2θ range 10–100°, by using 0.1° steps and 10 s counting time.

Results and Discussion

The nanocrystals were characterized by several techniques to assess their monodispersity, optical properties, lattice order, and purity.

The determination of nanocrystal size was the most delicate characterization, as the extinction coefficient would have been calculated from the volume of the nanocrystals, which depends on the third power of the radius. Small errors on the size would thus generate enormous errors on the extinction coefficient, thus invalidating the whole work. Therefore, the size of the nanocrystals was determined in independent ways by using different TEM and XRD analyses.

In the first case, the particle size determination was performed using both Z-contrast and high-resolution (HRTEM) imaging modes. The Z-contrast technique in scanning transmission electron microscopy (STEM) is very suitable for size determination of PbS nanocrystals. In fact, it provides an incoherent image of crystals where the intensity is proportional to the mean-square atomic number (Z^2),[33,34] and as consequence, the nanocrystals (deposited on a carbon film) display a white contrast on a black background. Moreover, the brightness variations are very low and can be easily flattened by subtracting the image background and introducing a threshold. For this reason, the standard software for particle size determination works well and allows analysis of a large number of PbS nanocrystals.

To check the absolute calibration and to avoid systematic errors in the thresholding operation, we have recorded on selected samples several photographs in HRTEM imaging mode: the PbS particles, showing a spherical shape, exhibit their crystalline nature that provides an internal reference for spatial calibration. The strong particle contrast allows easy detection of the border in such a way that the single-nanocrystal diameter can be measured with a good precision. To take into account the size dispersion, we have analyzed about 200–300 particles for each specimen; the size distribution was modeled with a Gaussian distribution, obtaining in this way the mean value, ranging from 4.24 ± 0.05 to 6.80 ± 0.05 nm. The polydispersity was found to range from ~6% to ~10%, with the smaller and larger samples being the most polydisperse, as expected from a nucleation and growth reaction involving focusing.[13] The low polydispersity of our samples is evident from Figure 1a,b, where a TEM image of nanocrystals dried on a grid and a HRSEM image of a nanocrystal superlattice are shown. No evidence of twinning or grain boundaries was detected in any of the characterized samples (see Figure 1c), leading to the conclusion of the "single crystal" nature of the nanoparticles.

Powder XRD techniques are largely applied to characterize the microstructure of polycrystalline materials. In particular, the Scherrer formula, giving the dependence of the "apparent" crystallite size from the additional broadening of the diffraction pattern, is widely used. It can be defined in the notation of Langford and Wilson[35] as

$$\epsilon = \frac{\lambda}{b \cos(\theta)}$$

where ϵ is the "apparent size" (the effective length along which diffraction is coherent, measured in the direction of the diffraction vector), λ is the wavelength of the X-ray radiation used, b is the "breadth" (a measure of the width of a Bragg reflection) in radians, and θ is the angle at which that reflection occurs. The true size of the crystallite, defined as the cube root of the crystallite volume, is given by $p = K\epsilon$, where K is a dimensionless number of the order of the unit, known as the

(33) Nellist, P. D.; Pennycook, S. J. *Ultramicroscopy* **1999**, *78*, 111–124.
(34) Nellist, P. D.; Pennycook, S. J. The principles and interpretation of annular dark-field Z-contrast imaging. In *Advances in Imaging and Electron Physics*; Academic Press Inc.: San Diego, 2000; Vol. 113, pp 147–203.
(35) Langford, J. I.; Wilson, A. J. C. *J. Appl. Crystallogr.* **1978**, *11*, 102–113.
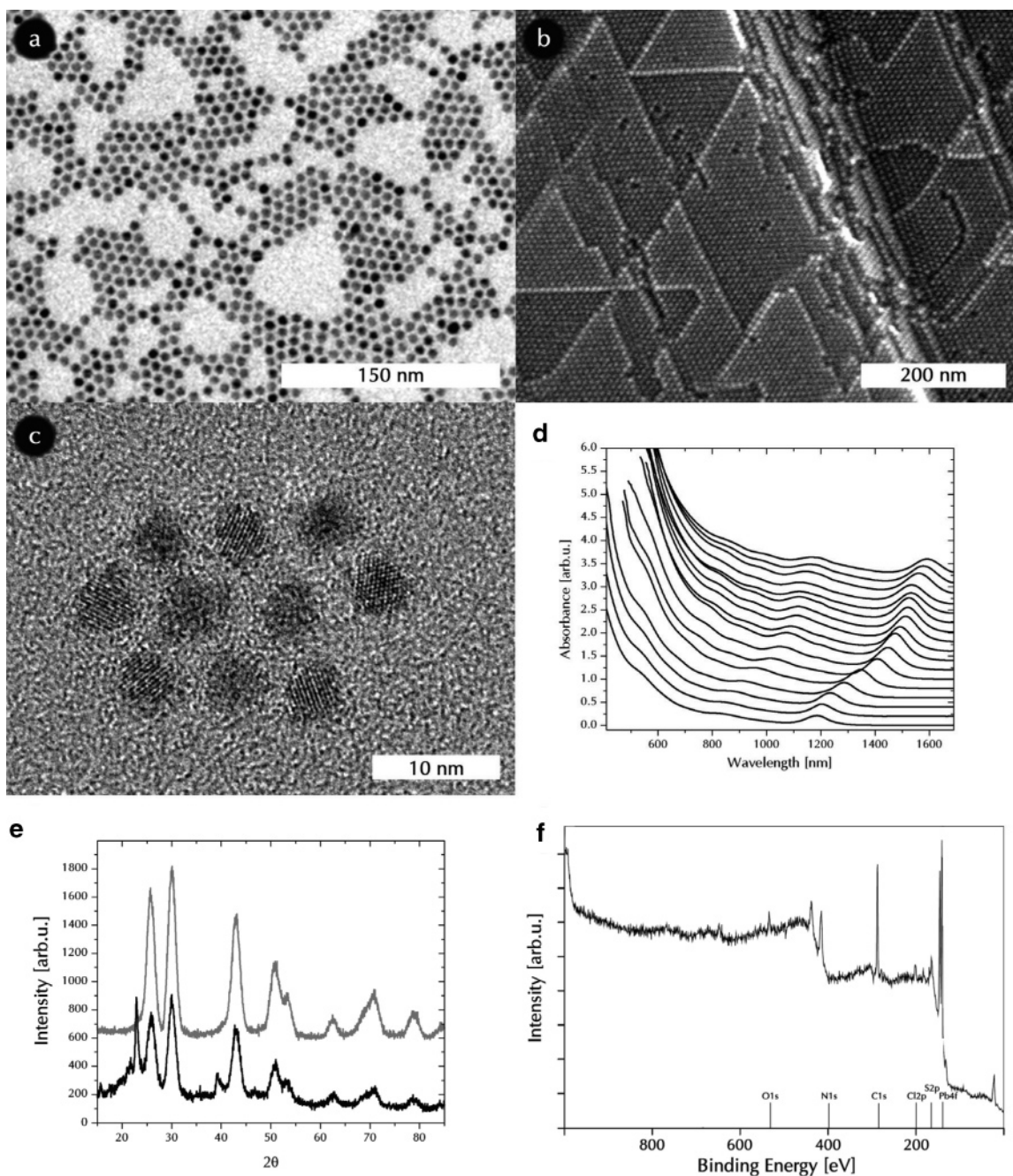
Figure 1. Characterization of PbS nanocrystals: (a) TEM image of a PbS nanocrystal; (b) HRSEM image of a PbS nanocrystal superlattice; (c) HRTEM micrograph of PbS nanocrystals showing crystallinity and absence of lattice defects; (d) absorption spectra of a size series of PbS nanocrystals (the spectra have been offset for clarity); (e) XRD spectra of films obtained from PbS nanocrystals with (gray solid line) and without (black solid line) purification with oleic acid; and (f) survey XPS spectrum of PbS nanocrystals.

Scherrer constant. The value of K depends on a variety of factors: the definition of "breadth" that is considered, the shape of the nanocrystals, and their size distribution. The latter are often unknown when the analysis is performed, so that the Scherrer formula is mostly used to give a rough estimation of the crystallite size, by taking a value $K = 0.90$ as a first approximation, as originally proposed by Scherrer.[36]

Besides the more traditional methods based on single-peak profile analysis, whole powder pattern fitting techniques (WPPF) like the Rietveld method[37,38] have also reached a significant maturity, especially when applied to microcrystalline samples.

However, when the particle size is in the range of few nanometers (as in the case of our PbS nanocrystals), sample effects (domain size, size distribution, particle shape, defects, etc.) can produce such broadened and overlapped peaks (and very often a complex peak shape) that the validity of the aforementioned methods may be strongly limited. Recently, many papers have been dealing with the problem using a *total* scattering approach, based on building up a 3D structural model of nanoparticles (NPs) of well-defined shape and size and using

(36) Sherrer, P. *Nachr. Ges. Wiss. Gottingen* **1918**, 26 September, 98.

(37) Balzar, D.; Audebrand, N.; Daymond, M. R.; Fitch, A.; Hewat, A.; Langford, J. I.; Le Bail, A.; Louer, D.; Masson, O.; McCowan, C. N.; Popa, N. C.; Stephens, P. W.; Toby, B. H. *J. Appl. Crystallogr.* **2004**, *37*, 911–924.

(38) Rietveld, H. M. *J. Appl. Crystallogr.* **1969**, *2*, 65.

the Debye function to compute the corresponding powder scattering pattern.[39−41] The Debye equation involves only the magnitude of interatomic distances, which means the calculation and the Fourier transform of the pair distance distribution function (PDF) of each cluster. The Debye formula, in its simplest form, is

$$I(k) = \sum_{i=1}^{N} \sum_{j=1}^{N} f_i f_j \frac{\sin(k r_{ij})}{k r_{ij}}$$

where $k = 4\pi \sin\theta/\lambda$ is the scattering vector, N is the cluster number of atoms, f_i and f_j are the atomic form factors (Debye−Waller factor included) of the ith and jth atoms, respectively, and r_{ij} is their distance.

For the PbS quantum dots under study, the analysis of the XRD patterns and the results of the SEM and TEM analyses convinced us to use the single-line Scherrer profile analysis to extract size information from the XRD data. Indeed, the (220) reflection appears to be not overlapping the neighbor reflections within a reasonable 2θ angular range, even in the experimental pattern of the smallest nanocrystals. The HRTEM observation of spherical nanocrystals makes acceptable the extraction of crystallite size information from a single reciprocal direction, K being the same for all the reflections. Moreover, the low observed polydispersity would account for a reduced dependence of the Scherrer constant from the size distribution. We decided to use the full width at half-maximum (fwhm) as a definition of breadth. For each dataset, the (220) peak was least-squares-fitted by using both a Pearson VII and a pseudo-Voigt function. In the first case, the background was subtracted and then the fwhm, the shape exponent, and the peak position were refined; in the second case, the fwhm, the Lorentzian/Gaussian fraction, the peak position, and the coefficient of a linear background were simultaneously refined. No significant difference was found in the fwhm results, except for the largest particle samples, for which the diffraction profile was probably influenced by a relatively larger polydispersity. In this case, the average value was considered. The values of p (the cube root of the nanocrystallite volume) were determined using the Scherrer formula by considering the calculated fwhm and assuming a Scherrer's constant $K = 0.829$, proposed for spherical crystallites[35] (this value holds only when the breadth is defined in terms of fwhm). The value of p^3 gave us the nanocrystallite volume, from which we calculated the nanocrystal radii r assuming the spherical shape using the following equation:

$$p^3 = {}^4/_3 \pi r^3$$

The diameters calculated from this application of the Scherrer formula, ranging from 4.16 ± 0.05 to 6.83 ± 0.05 nm, were found to lie within 3% of the TEM data (see Supporting Information). The same analysis performed on nonspherical nanocrystals gave bigger errors, thus confirming the sensitivity of K to the geometry of the crystallites.

Furthermore, to independently validate the size information using the whole experimental pattern, the Debye approach was applied. Still in agreement with the TEM observation about the shape of NPs, spherical-like clusters were generated (up to a diameter $D \approx 20$ nm) using the fcc crystal structure model of the corresponding bulk material and a shell-based building algorithm. The set of distances of each cluster was computed and then sampled according to a reported method,[42] to reduce the huge number of distances and save computing time for pattern calculation. Single-cluster simulations were compared to the diffraction data, aiming at assessing the average NPs size as estimated by the Scherrer formula. In fact, texture and/or surface roughness problems, affecting most of the experimental patterns, prevented — in the absence of suitable available corrections for the moment — applying a least-squares fitting procedure aimed at adjusting size distribution, strain, and thermal parameters, as previously reported.[40,41] In general, the agreement with the NP size determined by TEM and the Scherrer formula (within a few percent) can be considered satifactory. An example is shown in the Supporting Information, where the experimental pattern is compared with the calculated one, for which the cluster closest to the dimension determined by TEM and Scherrer analysis has been used. Having proven the reliability of this application of the Scherrer formula, we decided to use the diameters obtained from it for the further calculations related to the extinction coefficients.

The optical properties were probed by absorption spectroscopy. The first absorption peak could be tuned from 1186 to 1592 nm (see Figure 1d). The spectra featured multiple peaks, which provides further confirmation of the low polydispersity of the nanocrystals.

To verify the purity of the product, we conducted XRD measurements on samples after different steps of purification. Since the concentration of the nanocrystals would have been calculated from the ICP-AES results for Pb, we were concerned about possible traces of excess $PbCl_2$ still present in solution which would compromise the data. $PbCl_2$ forms a gel in oleylamine, but there is no knowledge about molecular precursors which might form in the conditions used for this experiment. The $PbCl_2$−OLA gel precipitates once the reaction is quenched into cold hexane, a process that sometimes takes a considerable amount of time. For this reason, the nanocrystals were characterized only months after their synthesis in order to be sure that all $PbCl_2$ had precipitated. We then characterized the sample via XRD to detect traces of $PbCl_2$ in the samples, even in the form of nanocrystallites. In Figure 1e, we have plotted the XRD results from samples obtained after different stages of purification. XRD spectra collected from samples that were not exposed to OA during the purification procedure showed the presence of residual $PbCl_2$ (Figure 1e, black solid line). The samples that were treated with OA during the purification were instead clean and phase-pure (Figure 1e, gray solid line).

Even though $PbCl_2$ is removed from the system, chlorine is still detected by XPS in quantities which are compatible with a monolayer of chloride ions on the surface of the nanocrystals[13] (see Figure 1f). The HRTEM was unable to detect the presence of any crystalline shell on the material, thus suggesting the

(39) Zanchet, D.; Hall, B. D.; Ugarte, D. *J. Phys. Chem. B* **2000**, *104*, 11013−11018.
(40) Cervellino, A.; Giannini, C.; Guagliardi, A. *J. Appl. Crystallogr.* **2003**, *36*, 1148−1158.
(41) Cervellino, A.; Giannini, C.; Guagliardi, A.; Zanchet, D., *Eur. Phys. J. B* **2004**, *41*, 485−493.

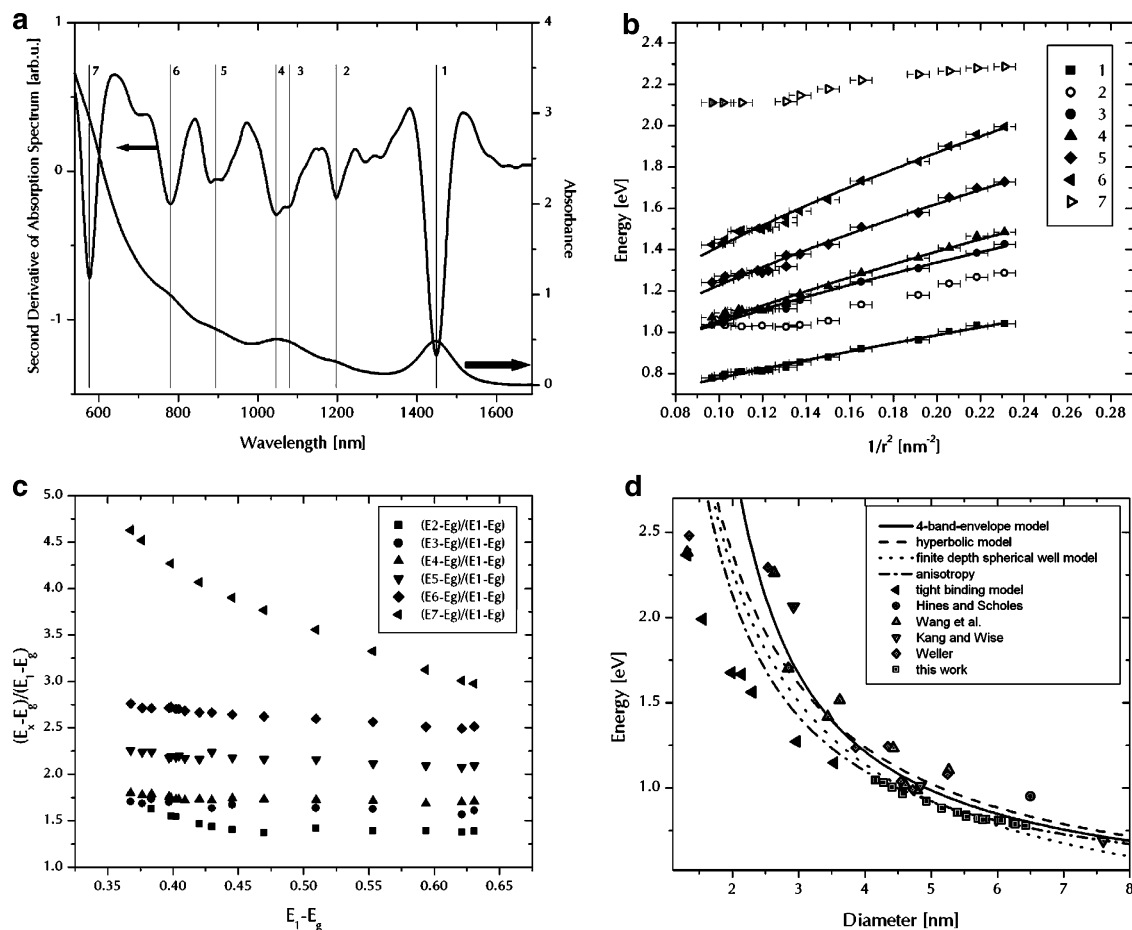(42) Cervellino, A.; Giannini, C.; Guagliardi, A. *J. Comput. Chem.* **2006**, *27*, 995.

Figure 2. Absorption spectroscopy of PbS colloidal nanocrystals: (a) second-derivative analysis of the absorption spectrum; (b) plot of transition energies versus r^{-2}, showing the seven different transition identified (equations for the fits are given in the text); (c) exciton confinement energies as a function of the first exciton confinement energy; and (d) plot of the energy of the $1S_e-1S_h$ transition versus size, comparing computational data (lines and black triangles) and experimental data (gray scatters) from different sources.

chloride ions might be chemisorbed on the surface. PbCl$_2$ is insoluble in oleylamine, suggesting that the Cl$^-$ ions might remain bound to Pb until they are displaced by S. This displacement might be incomplete for the surface Pb atoms, creating a "shell" of chemisorbed chloride ions which are kept in place by the apolarity of the solvent. The presence of these ions on the surface would also promote the stabilization of Pb-terminated surfaces, explaining the unusual resistance of the luminescence of these nanocrystals toward oxidation.[43]

A second-derivative analysis of the absorption spectra (Figure 2a) allowed us to clearly identify seven transitions and the dependence of their energy on the size of the nanocrystals. Since it is known that this sort of analysis can easily yield spurious peaks, we assigned a transition only to those peaks that were reproducibly found in the vast majority (at least two-thirds) of the spectra we collected and that were clearly slowly shifting with changing size of the nanocrystals. Especially considering the reasonably large number of samples analyzed, these criteria looked, to us, to be the best and most accurate solution. In particular we plotted in Figure 2b the transition energies versus the inverse square radius. The data have been fitted with an equation representing the major energetic terms defining the transition energies: bulk band gap energy (constant), quantum confinement energy (proportional to $1/r^2$), and Coulomb at-

traction (proportional to $1/r$).[6] The spatial correlation term was left out in consideration of the high dielectric constant of our material.[6] The fits obtained were reasonably good (correlation coefficient > 0.99). The equations for the best fits are given as follows:

$$E_1 \ (\text{eV}) = 0.41 + 0.96/r^2 + 0.85/r$$

$$E_3 \ (\text{eV}) = 0.41 + 0.54/r^2 + 1.83/r$$

$$E_4 \ (\text{eV}) = 0.41 + 1.15/r^2 + 1.67/r$$

$$E_5 \ (\text{eV}) = 0.41 + 0.93/r^2 + 2.29/r$$

$$E_6 \ (\text{eV}) = 0.41 + 0.67/r^2 + 2.97/r$$

Two transitions, numbers 2 and 7, could not be fitted with the same equation, and their identification is troublesome. They appear consistently in every spectra, and they shift in energy with size, thus excluding the possibility that they come from impurities or excess precursors in the solution. Transition 7 might come from magic number clusters present in solution, but in such a case it would not shift in energy and its profile would be sharper.

In the effective mass approximation, the normalized confinement energies for each transition should remain constant for

(43) Cademartiri, L.; von Freymann, G.; Arsenault, A. C.; Bertolotti, J.; Wiersma, D. S.; Kitaev, V.; Ozin, G. A. *Small* **2005**, *1*, 1184−1187.

comparable degrees of confinement. By "normalized confinement energy", we mean the confinement energy of a transition $(E_x - E_g)$ divided by the confinement energy of the first exciton $(E_1 - E_g)$.[44] A plot of these quantities as a function of the confinement energy of the first exciton is given in Figure 2c. For every transition save the seventh, and in small part the second, the normalized confinement energies are nearly constant at the following values, with a confidence interval of 99.7%:

$$\langle (E_2 - E_g)/(E_1 - E_g)\rangle = 1.39 \pm 0.06$$

$$\langle (E_3 - E_g)/(E_1 - E_g)\rangle = 1.7 \pm 0.1$$

$$\langle (E_4 - E_g)/(E_1 - E_g)\rangle = 1.73 \pm 0.09$$

$$\langle (E_5 - E_g)/(E_1 - E_g)\rangle = 2.2 \pm 0.1$$

$$\langle (E_6 - E_g)/(E_1 - E_g)\rangle = 2.6 \pm 0.2$$

These values allow us to assign, with a fair confidence, the transitions to the individual energy levels in the electronic structure of the quantum dots. By using the energy levels calculated by Tudury et al.,[45] we found that transition 2 could be assigned to $1S_e–1P_h$ (or $1P_e–1S_h$), and transition 3 and 4 can both be assigned to $1P_e–1P_h$, with different values of *j*. The attribution of the equivalent of transition 2 in PbSe transition is becoming less controversial, as more and more experimental data and simulations are gathered supporting this conclusion.[22,46] Transition 2 would be, in fact, parity-forbidden, and its appearance could be due to the band anisotropy of lead chalcogenides,[1] to permanent dipole moments,[47,48] or to intervalley scattering.[46] In the anisotropy framework, the fact that the oscillator strength of this transition is much weaker than in PbSe can be explained by the weaker anisotropy of PbS compared to PbSe.[21] The weakness of our attribution of transition 2 lies in the fact that the normalized confinement energy for that transition is not constant for the largest dots we characterized but is increasing with size, as can be seen in Figure 2c. The true identity of this transition is then still controversial, but we hope these data might help to shed some light on it.

The $1S_e–1S_h$ transition is easier to model and to measure experimentally. In Figure 2d, we plotted all the available simulations and experimental data we could find on the energy of the $1S_e–1S_h$ transition as a function of size for PbS nanocrystals. Simulations are lines (except for the tight binding model, which is represented by black triangles), while experimental data are gray symbol scatters. The experimental data we took from the literature are widely scattered on the graph, probably because of sample polydispersity, different sizing methods, or different synthetic procedures. Our data are indicated by the gray squares. Very interesting is the comparison with the simulations. The black solid line is taken from the four-band-envelope model developed by Kang and Wise,[49] and it seems to overestimate the energies when compared to our data.

The dashed black line represents the hyperbolic band model developed by Wang et al.,[4] which was also found to overestimate the transition energies found in our samples. The dotted line represents the finite-depth spherical well model developed by Nosaka,[50] which estimates very well the absolute values of the transition energies we found but not so much their dependence on the size. The tight binding model,[51] represented by the black triangles, as expected, underestimates the transition energies, even though we cannot directly compare its values with our values since the size ranges are not overlapping. The best fit of our data was obtained by a four-band envelope model formulated by Andreev and Lipovskii[1] (and shortly thereafter extended by Tudury et al.[45]) to take into account the band anisotropy of lead chalcogenides (dash-dotted line in Figure 2d). The quality of the agreement is striking, as it almost perfectly matches the absolute values as well as the size dependence. It is not clear at this point if this good agreement is due to the inclusion of anisotropy in the calculation: the paper from Tudury et al.[45] shows that the effect of anisotropy on the first transition energy is in fact minimal for PbS; very similar calculations done by Andreev and Lipovskii[1] show instead a relevant shift of the $1S–1S$ transition energies to lower values, consistent with what was observed by comparing our data with the four-band envelope model of Kang and Wise, in which anisotropy was introduced as a perturbation; similar results reported by Ellingson et al.[22] for PbSe seemed to show that the anisotropy did not need to be included in the calculation, at least for the first transition energy. It is likely also that the different parameters used in the calculations might have had a consistent effect on the agreement with the experimental data reported here. To further support this agreement, it is important to extend the size range obtainable via our synthesis, and experiments with this purpose are underway.

Transition 7 remains difficult to interpret, especially given its different dependence on size. We suggest here that this transition might be the interband transition along the Σ direction. This transition, which has been labeled as E_1 in the past literature,[52–54] has an energy close to the energy we measured for transition 7, especially for the larger nanocrystals.

The extinction coefficients have been calculated using data from Scherrer analysis of XRD spectra, and Pb concentrations given by ICP-AES analysis. A solution with a known absorption spectrum was dried, digested with $HNO_3–H_2O_2$ mixture, diluted with Millipore water, and analyzed for Pb concentration using ICP-AES. From the obtained Pb concentrations, we calculated the volume of PbS in the original solution, which was then divided by the volume of a single nanocrystal, by using the radii obtained from Scherrer analysis and assuming the nanocrystals to be perfect spheres. We then obtained the number of nanocrystals, which, when divided by the volume of the original solution in hexane, gave us the concentration of the nanocrystals. The extinction coefficients were then obtained from the absorbance and the concentration of nanocrystals by using the Beer–Lambert law. The absorbance at the $1S_e–1S_h$ maximum was kept in the linear regime of absorption. We made sure to avoid

(44) Wehrenberg, B. L.; Wang, C.; Guyot-Sionnest, P. *J. Phys. Chem. B* **2002**, *106*, 10634–10640.
(45) Tudury, G. E.; Marquezini, M. V.; Ferreira, L. G.; Barbosa, L. C.; Cesar, C. L. *Phys. Rev. B* **2000**, *62*, 7375.
(46) Allan, G.; Delerue, C. *Phys. Rev. B* **2004**, *70*.
(47) Shim, M.; Guyot-Sionnest, P. *J. Chem. Phys.* **1999**, *111*, 6955–6964.
(48) Cho, K. S.; Talapin, D. V.; Gaschler, W.; Murray, C. B. *J. Am. Chem. Soc.* **2005**, *127*, 7140–7147.
(49) Kang, I.; Wise, F. W. *J. Opt. Soc. Am. B* **1997**, *14*, 1632–1646.

(50) Nosaka, Y. *J. Phys. Chem. B* **1991**, *95*, 5054.
(51) Kane, R. S.; Cohen, R. E.; Silbey, R. *J. Phys. Chem.* **1996**, *100*, 7928–7932.
(52) Cardona, M.; Greenaway, D. L. *Phys. Rev. A* **1964**, *133*, 1685.
(53) Kohn, S. E.; Yu, P. Y.; Petroff, Y.; Shen, Y. R.; Tsang, Y.; Cohen, M. L. *Phys. Rev. B* **1973**, *8*, 1477–1488.
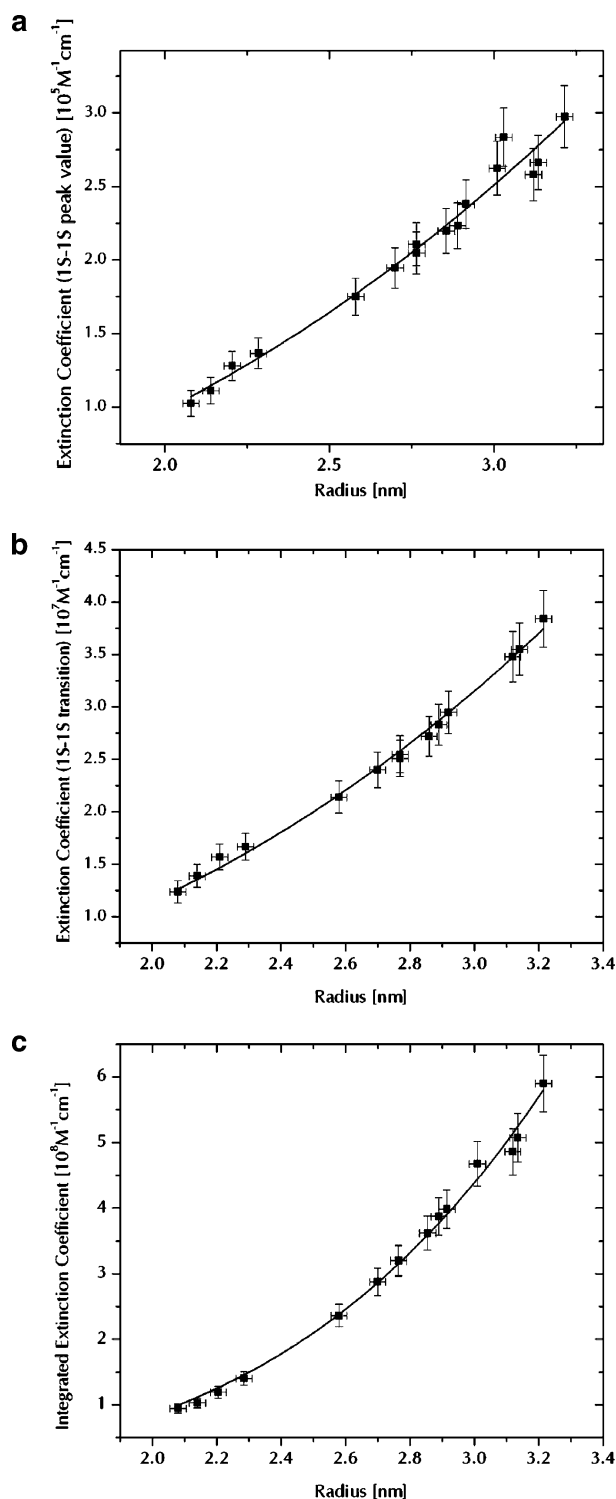(54) Kanazawa, H.; Adachi, S. *J. Appl. Phys.* **1998**, *83*, 5997.

Figure 3. Extinction coefficient of PbS nanocrystals. The lines are power law fits, the equations of which are given in the text. (a) Extinction coefficient of the $1S_e-1S_h$ transition, calculated using the peak value of absorbance; (b) integrated extinction coefficient of the $1S_e-1S_h$ transition; and (c) extinction coefficient integrated from 555 nm.

particle aggregation due to dilution, which would have altered the data. Nanocrystals tend to lose their colloidal stability in very pure and dilute solutions, causing the formation of aggregates.

The plots of the size dependence of the extinction coefficients are shown in Figure 3. The extinction coefficients obtained from

the peak value of the $1S_e-1S_h$ transition are plotted in Figure 3a as a function of nanocrystal radius. The data were fitted with a power law with the following values of the parameters:

The extinction coefficient of the $1S_e-1S_h$ transition was

$$\epsilon\,(M^{-1}\,cm^{-1}) = 19600r^{2.32} \qquad \text{with } R^2 = 0.98$$

obtained by integrating the extinction coefficient over the low-energy side of the peak and multiplying the value by 2. The obtained values as a function of the nanocrystal radius are given in Figure 3b. The data were fitted with a power law as follows:

The extinction coefficient was also integrated starting from

$$\epsilon\,(M^{-1}\,cm^{-1}) = 2030790r^{2.49} \qquad \text{with } R^2 = 0.995$$

555 nm, giving the data shown in Figure 3c. The line is a power law fit, obtained as follows:

$$\epsilon\,(M^{-1}\,cm^{-1}) = 5149146r^{4.05} \qquad \text{with } R^2 = 0.994$$

All the r values in the formulas are expressed in nanometers. The errors on the exponents are about 3%, while the errors on the coefficients are about 6%. We must, however, warn the reader that, even though we took every possible precaution to reduce errors, there are still many potential sources of error which are extremely difficult to estimate. For example, in the calculation of the concentration of nanocrystals from the ICP-AES data, we assumed the nanocrystalline PbS to have the same density as the bulk material; to be precise, even though this should be a good approximation, it is not true due to lattice relaxation at the surface. Also, the error on the size determination is extremely small (± 0.05 nm), which is a consequence of the least-squares fitting of the XRD patterns, which were very dense. This deviation might be underestimated, but we decided to keep it, as considering sources of error which are not rigorously quantifiable would make the resulting data more questionable. In all the graphs in Figure 3, the errors have been calculated by propagating all the known errors for each quantity used for the calculations. For extinction coefficients, the relative errors are between 7% and 8.5%. Also, fitting these data with a power law is not justified a priori. These fits are just a way to quantify, in a simple way, the extent of size dependence and to compare it with previous literature. It is then not suggested to extrapolate these fits out of the size range explored herein.

Consistent with the results reported by Yu et al.,[29] the size dependence of the extinction coefficient of the lowest energy transition follows a power law with exponent between 2 and 3. The most significant data are the ones obtained from the integration of the $1S_e-1S_h$ transition. Their values, in fact, should be independent of polydispersity of the sample, as also suggested by the improved quality of the fit when compared to the extinction coefficient calculated from the peak value. We thus suggest that the reader use those values to calculate the concentration of a PbS nanocrystal dispersion.

The *per particle* absorption cross sections can be calculated easily from the extinction coefficient[26] by using

$$C_{abs} = \frac{2303}{N_A}\epsilon$$

where N_A is Avogadro's number, giving for the $1S_e-1S_h$ peak
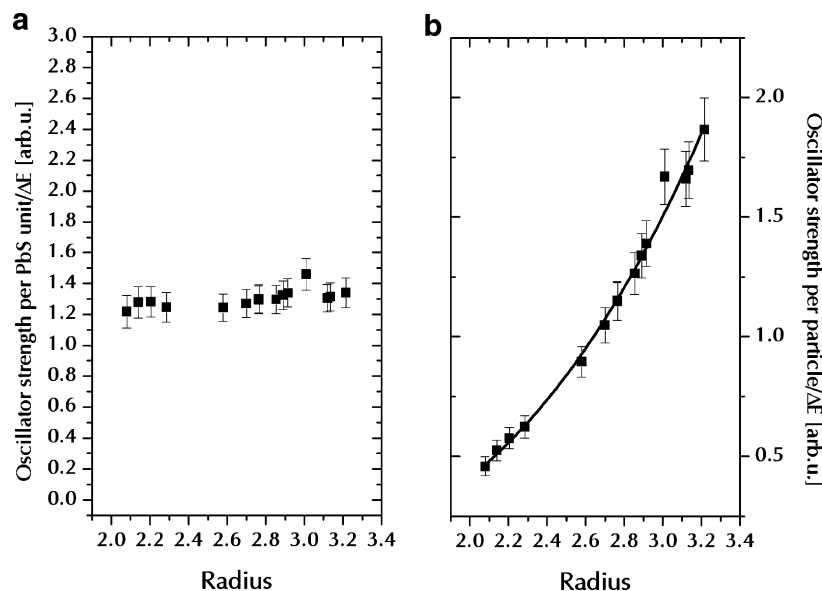
Figure 4. Size dependence of the transition-energy-normalized oscillator strength for the 1S−1S transition: (a) *per unit* oscillator strength, showing little or no size dependency, and (b) *per particle* oscillator strength, as a function of nanocrystal radius. The black line is a power law fit with exponent equal to 3.20.

value of the *per particle* absorption cross section

$$C_{abs} = 7.494 \times 10^{-17} r^{2.31}$$

for the *per particle* absorption cross section, integrated over the $1S_e-1S_h$ transition,

$$\int_{1S1S} C_{abs} = 7.196 \times 10^{-15} r^{2.58}$$

and for the *per particle* absorption cross section, integrated from 555 nm,

$$\int_{555}^{\infty} C_{abs} = 1.969 \times 10^{-14} r^{4.22}$$

The oscillator strength for the exciton *per PbS unit* is given by

$$f = \frac{2m}{\hbar} \Delta E |\mu|^2 |U(0)|^2$$

where m is the electron mass, ΔE is the transition energy, μ is the dipole moment of the transition, and $U(0)$ is the probability of finding the electron and hole in the same unit volume.[6] In conditions of strong quantum confinement, the oscillator strength would then increase with a decrease in particle size due to the increasing overlap between electron and hole wave functions.[6,26] This increase would be almost exactly compensated in the *per particle* oscillator strength, as the number of units decreases with decreasing particle size.[6,26] So, the main prediction,[6,26] according to the effective mass approximation, neglecting Coulomb interactions and ΔE dependence, is that the *per particle* oscillator strength for the lowest energy transition should be nearly size independent, while the oscillator strength *per unit* should scale with $1/R^3$. As shown in Figure 4, this picture is not too well reproduced by our experimental results. In the left panel we show the *per unit* oscillator strength divided by the transition energies plotted against the radius, showing no significant dependence on size. On the right panel we instead show the *per particle* oscillator strength also normalized against transition energies, showing a strong dependence on size which

could be represented by a power law with exponent equal to 3.20 ($R^2 = 0.995$). It is striking that the *per unit* oscillator strength remains almost constant, especially considering the extreme degree of quantum confinement experienced in lead chalcogenide quantum dots.

The strong dependence on size of the *per particle* absorption cross section is consistent with the report of Yu et al.[29] but not consistent with other reports, in which no dependence[32] or a linear dependence[26] was seen. There might be several reasons for this. We argue that, considering the technical difficulty of the measurement, the discrepancies are mostly attributable to the different protocols and methodologies employed (especially in the sizing techniques). For example, our size dependence could be reasonably well fitted with a line if the number of samples was even slightly more limited. We then hope that these results and the sizing protocol proposed here will help and convince other scientists to explore their quantum dot system to confirm or disprove the generality of this size dependency of the extinction coefficients.

Conclusions

We have reported here a detailed study on the transition energies and extinction coefficients of PbS nanocrystals in the range of sizes between 4 and 7 nm. A synergic use of XRD and TEM characterization allowed us to determine the sizes of the nanocrystals with good precision, obtaining nearly identical values by different techniques. The low polydispersity of the samples allowed us to investigate seven transitions and their size dependence. The size dependence of the transition energies was found to be best simulated by a four-band envelope model which accounts for band anisotropy.[1,45] The extinction coefficients were measured using elemental analysis techniques, and their size dependence was measured under several conditions. The extinction coefficient and the *per particle* absorption cross section, integrated over the $1S_e-1S_h$ transition, were found to depend on nanocrystal size according to a power law with an exponent of ∼2.5. The errors in the measurement of the extinction coefficient were propagated by considering all known

sources of error and were found to be less than 10%. We are confident that these measurements will be of great use for the many future applications and studies involving PbS nanocrystals in which knowledge of their concentration in solution will be necessary, especially considering the extraordinary properties of these materials.[17,19,20,22]

Supporting Information Available: Comparison of sizing data from Scherrer analysis and TEM analysis (Figure S1); XRD pattern fitting with Debye method (Figure S2). This material is available free of charge via the Internet at http://pubs.acs.org.

JA063166U